Nuclear Instruments and Methods in Physics Research A 764 (2014) 352–368

Contents lists available at ScienceDirect

Nuclear Instruments and Methods in Physics Research A

journal homepage: www.elsevier.com/locate/nima

Future hadron colliders: From physics perspectives to technology R&D ☆

William Barletta [a,b], Marco Battaglia [c,d,e,*], Markus Klute [b], Michelangelo Mangano [e], Soren Prestemon [d], Lucio Rossi [e], Peter Skands [e]

[a] Department of Physics & Astronomy, University of California at Los Angeles, CA 90095, USA
[b] Department of Physics, Massachusetts Institute of Technology, Cambridge, MA 02139, USA
[c] Santa Cruz Institute of Particle Physics, University of California at Santa Cruz, CA 95064, USA
[d] Lawrence Berkeley National Laboratory, Berkeley, CA 94720, USA
[e] CERN, CH-1211 Geneva, Switzerland

ARTICLE INFO

Article history:
Received 22 January 2014
Received in revised form
23 June 2014
Accepted 4 July 2014
Available online 24 July 2014

Keywords:
Future hadron colliders
Superconducting magnet technology
High energy proton beams

ABSTRACT

High energy hadron colliders have been instrumental to discoveries in particle physics at the energy frontier and their role as discovery machines will remain unchallenged for the foreseeable future. The full exploitation of the LHC is now the highest priority of the energy frontier collider program. This includes the high luminosity LHC project which is made possible by a successful technology-readiness program for Nb_3Sn superconductor and magnet engineering based on long-term high-field magnet R&D programs. These programs open the path towards collisions with luminosity of 5×10^{34} cm^{-2} s^{-1} and represents the foundation to consider future proton colliders of higher energies. This paper discusses physics requirements, experimental conditions, technological aspects and design challenges for the development towards proton colliders of increasing energy and luminosity.

Contents

☆This review is based on the final report of the Frontier Capabilities Hadron Collider Study Group at the APS Community Summer Study – CSS 2013.

* Corresponding author.
E-mail addresses: MBattaglia@lbl.gov, battaglia@scipp.ucsc.edu (M. Battaglia).

http://dx.doi.org/10.1016/j.nima.2014.07.010
0168-9002/

1. Introduction

High energy hadron colliders have been the tools for discovery at the highest mass scales of the energy frontier from the S$\overline{\text{p}}$pS, to the Tevatron and now the LHC. They will remain so, unchallenged for the foreseeable future. The discovery of the Higgs boson at the LHC [1,2] opens a new era for particle physics. After this discovery, understanding what is the origin of electro-weak symmetry breaking becomes the next key challenge for collider physics. This challenge can be expressed in terms of two questions: up to which level of precision does the Higgs boson behave like predicted by the SM? Where are the new particles that should solve the electro-weak (EW) naturalness problem and, possibly, offer some insight into the origin of dark matter, the matter–antimatter asymmetry, and neutrino masses? The approved CERN LHC programme, its future upgrade towards higher luminosities (HL-LHC) [3], and the study of either an LHC energy upgrade (HE-LHC) [4] or a new proton collider delivering collisions at a centre of mass energy up to 100 TeV (FCC-hh) [5], are all essential components of this endeavour, as discussed in Section 2.

LHC is expected to restart in Spring 2015, colliding protons at centre-of-mass energies of 13–14 TeV and its design luminosity of $10^{34}\,\text{cm}^{-2}\,\text{s}^{-1}$ to be reached in the course of the year. After 2020, some critical components of the accelerator will reach the radiation damage limit and others will have reduced reliability, also due to radiation effects. At the same time the statistical gain in running the collider at constant luminosity will progressively decrease and the LHC will need a decisive increase of its luminosity to continue expanding its probe to new phenomena and higher mass scales [6,7]. This new phase of the LHC life, named the High Luminosity LHC (HL-LHC), will prepare the machine to attain the astonishing threshold of 3000 fb^{-1} of integrated luminosity during its first decade of operation [8]. High-luminosity offers the potential to increase the precision of several key LHC measurements, to uncover rare processes, and to guide and validate the progress in theoretical modelling, thus reducing the systematic uncertainties in the interpretation of the data. The project is now the first priority of Europe, as stated by the Strategy Update for High Energy Physics approved by the CERN Council [9].

The single most critical technology, underlying the LHC and proton colliders beyond the present LHC configuration, is super-conducting (SC) magnet technology. Indeed, the present LHC is based on ~40 years of development of SC technology using NbTi wire. In the LHC, its NbTi-based magnets are pushed to their limits both in the collider arcs and in the interaction regions. The preferred route towards the increased luminosity for the HL-LHC upgrade is the reduction of the β^* parameter of the beam optics, controlling the beam focusing at the interaction point (IP), by means of larger aperture triplet magnets in the interaction region. This design requires quadrupoles with an aperture of 150 mm and peak field in excess of 12 T, beyond the capabilities of the NbTi conductor. Therefore, it relies heavily on the success of the advanced Nb_3Sn SC technology, which has the advantage of a critical field a factor of two higher compared to NbTi and was developed by the US LHC Accelerator Research Program (LARP) [10]. The success of the HL-LHC project will be pivotal in demonstrating the viability of Nb_3Sn technology for collider applications. The development of the SC technology towards high magnetic fields is discussed in Section 5.

In the exploration of the energy frontier with hadron collisions, energy and luminosity play a complementary role. In reaching toward higher energies, magnet technology will retain its central role. In addition to the focused program of engineering development, the separate programs of long range research in magnet materials and structures are of crucial importance. It was these programs which have provided the intellectual and infrastructure base for the success of the Nb_3Sn magnet development. For the long range future of high energy physics using pp collisions, advances in magnets with operating fields of 14–16 T, or beyond, will be needed. Given the progress in magnet technology and the maturity that Nb_3Sn has reached, it is legitimate to forecast that Nb_3Sn magnets can reach their limit of 14–16 T in operating conditions within the next decade, opening the path towards a collider with energy significantly larger than that of the LHC and an exceptional potential for probing the energy frontier farther. High-temperature superconductor (HTS) materials are under investigation for even higher field magnet applications. In practice, the decision on the SC technology will rest on a tradeoff between tunnel cost, which scales roughly inversely with dipole field, and the cost of the dipole magnets, whose cost-scaling with field is roughly linear when operated far from the conductor critical field B_{c2}, but more complex as the operating point approaches the B_{c2} limit. The crossover in cost cannot be decided *ab initio*, as the tunnel cost will depend strongly on the geology of the chosen site [11].

With the renewed interest in a ~100 TeV scale collider [12], the design study for a machine in a large tunnel becomes topical. The beam momentum reach of a collider, p, is directly proportional to the magnetic dipole field strength, B, and the tunnel radius R. The construction of a new tunnel relieves the pressure from the achievable dipole field strength, since this can be traded for the tunnel circumference. The target collision energy of a future circular hadron collider (FCC-hh) is 100 TeV for 20 T dipoles, based on HTS wire, in an 80 km tunnel. However, a 100 km tunnel would provide the same collision energy of 100 TeV with reduced field of 14–16 T, reachable with Nb_3Sn technology that relies on a much more mature and less expensive conductor than HTS. The 100 TeV collider study will inform directions for expanded technology reach and help guide the long-term roadmap of high energy physics capabilities. Areas of particular value to the R&D portfolio include studies of beam dynamics, magnets, vacuum systems, machine protection and global layout optimisation. We note that a large tunnel may also open up the possibility of an e^+e^- storage ring [13,14], of interest as a Z, W and Higgs factory, if the International Linear Collider is not built, and of e^-p collisions. The options of a collider housed in the LHC tunnel (HE-LHC) and that in a new, larger tunnel (FCC-hh) are presented in Section 6.

Whether in the LHC tunnel or in a new, larger tunnel, a collider with energy beyond that of the LHC will have to deal with an additional challenge, the emission of beam synchrotron radiation at a rate per unit of length at least 20 times greater compared to the LHC at its nominal parameters, as discussed in Section 6. The beam pipe and beam screen will have to absorb that radiation. Although synchrotron radiation is very beneficial for beam stabilisation and will make such a high energy collider the first hadron machine dominated by synchrotron radiation damping, the power dissipated in synchrotron radiation must be removed at cryogenic temperatures. In the LHC, this is removed at 5–10 K. Merely relying on a solution similar to that adopted at the LHC, with a beam screen at 10 K, would be a heavy burden for the cryogenics. For the HE-LHC, a solution based on a beam screen at 40–60 K has been

envisaged and has no major drawback, although careful design, engineering and prototyping need to be developed to prove this solution. For a ~100 TeV machine, handling the synchrotron radiation will become a major challenge, requiring a detailed study.

2. The physics landscape

The observation of the Higgs boson at the LHC opens a new era for particle physics. Its measured properties are consistent, within the current uncertainties, with those of the Standard Model (SM) Higgs boson. This gives a remarkable confirmation of the theoretical setup, formulated over forty years ago, to explain the otherwise inconsistent co-existence of a gauge theory for electro-weak (EW) interactions, with the masses of the gauge bosons, quarks and charged leptons. On the other hand, the complete lack of evidence for new physics makes the understanding of the naturalness of the EW scale more concrete and urgent. The smallness of the EW scale compared to the Planck scale requires, in the context of the SM, an incredible amount of fine tuning. This is an intrinsic problem of the SM, generally referred to as the "hierarchy problem". The existence of new physics beyond the SM (BSM) is also needed in view of the SM inadequacy to explain a number of intriguing phenomena, like dark matter, the matter–antimatter asymmetry and neutrino masses.

After the discovery of the Higgs boson, understanding what is the real origin of EW symmetry breaking (EWSB) becomes the next key challenge for collider physics. This challenge can be expressed in terms of two questions: up to which level of precision does the Higgs boson behave as predicted by the SM? Where are the new particles that should solve the EW naturalness problem and, possibly, offer some insight in the origin of dark matter, the matter–antimatter asymmetry, and neutrino masses? The first question allows us to define concrete deliverables for the LHC and future colliders. We know there is a Higgs boson at a mass of about 125 GeV and we can thus analyse in great detail the prospects for more precise measurements of all of its properties at the various facilities. The second question does not come with the guarantee of concrete discovery deliverables, but its relevance is powerful enough to justify pursuing the search efforts as ambitiously as possible.

The approved LHC programme, its future upgrade towards higher luminosities, and the study for a new hadron collider delivering collisions at significantly higher energy, are all essential components of the particle physics endeavour at the energy frontier. High-luminosity offers the potential to increase the precision of several key measurements, to uncover rare processes, and to guide and validate the progress in theoretical modelling, thus reducing the systematic uncertainties in the interpretation of the data. The extended lever arm afforded by an higher collision energy increases the potential to directly probe greater and greater mass scales for BSM processes, and gives access to the TeV energy scale, which is the natural domain to test the dynamics of EWSB (e.g. high-mass WW→WW and WW→HH scattering, triple and quartic gauge and Higgs couplings). Detailed studies of the realistic performance in the measurements of Higgs couplings, self-coupling and WW scattering at energies above 14 TeV do not yet exist and will be required to precisely assess their accuracy and potential. More in general, higher statistics, whether coming from higher luminosity or from increased cross-sections at higher energies, open new opportunities for both searches and measurements, enabling analysis strategies where tighter cuts can greatly improve the signal purity and/or reduce the theoretical uncertainties. The long history of the Tevatron gives clear evidence of the immense progress that can be made, relative to naive earlier estimates, after the accumulation of bigger amounts of data and of more experience with their analysis.

Table 1
Evolution of the cross-sections for different Higgs production processes in pp collisions with centre-of-mass energy The cross-sections at $\sqrt{s} = 14$ TeV are given in the second column, and the ratios $R(E) = \sigma(E\ \text{TeV})/\sigma(E = 14\ \text{TeV})$ in the following columns. All rates assume $M_H = 125$ GeV and SM couplings.

Process	σ (14 TeV)	R (33)	R (40)	R (60)	R (80)	R (100)
gg→H	50.4 pb	3.5	4.6	7.8	11	15
qq→qqH	4.40 pb	3.8	5.2	9.3	14	19
$q\bar{q}$→WH	1.63 pb	2.9	3.6	5.7	7.7	10
$q\bar{q}$→ZH	0.90 pb	3.3	4.2	6.8	10	13
pp→HH	33.8 fb	6.1	8.8	18	29	42
pp→ttH	0.62 pb	7.3	11	24	41	61

The lack of a guarantee that *any* future facility will directly observe new particles greatly strengthens the relevance of a broad programme of very precise measurements. The exploration of the Higgs sector provides us with a benchmark for the assessment of the physics potential of future facilities, including hadron colliders at the energy frontier. Several directions should be pursued, including the high-precision study of the couplings already observed, the search of rare (e.g. H→$\mu^+\mu^-$) or forbidden Higgs decays and the study of the dynamics of Higgs interactions, including Higgs-pair production processes, sensitive to the Higgs self-coupling and to possible anomalous interactions.

What really defines the Higgs boson is its role in breaking the EW symmetry, in particular, its coupling to the longitudinal polarisation of W and Z bosons and the resulting unitarization of high-energy WW scattering. This is a key element in the study of EWSB. The theoretical description of WW scattering requires the exchange of the Higgs boson, or of some other new particle, in order to tame the otherwise unphysical rate growth at energies around the TeV and above. Verifying the details of this process is essential to learn more on whether the Higgs boson is indeed a fundamental particle or, as postulated in some theories, a composite object, something that could also manifest itself with the appearance of new resonances in the TeV range. These studies require the highest possible energies to probe the relevant mass scales. For example, in a class of composite-Higgs models, deviations from the SM behaviour of the WW scattering cross-section, due to anomalous Higgs interactions, scale like $\xi^2(E_{CM}(\text{WW})/600\ \text{GeV})^4$, where ξ is related to the scale of new physics,[1] and determines also a change of order ξ, w.r.t. the SM prediction, in BR (H→WW*). It takes centre-of-mass energies of the WW system well above 1 TeV to have sensitivity to these deviations. At 14 TeV and 300 fb^{-1}, the statistics of events with $E_{CM}(\text{WW}) > 1$ TeV is limited and experiments will only be sensitive to values $\xi \gtrsim 0.5$. This sensitivity improves to ξ values of $\mathcal{O}(0.10)$ and $\mathcal{O}(0.01)$ for pp collisions at 30 and 100 TeV, respectively. The design energy of the SSC, 40 TeV, was chosen to optimise the reach and precision of these measurements. The need to perform these studies today is even stronger than it was in the days of the SSC planning, due to the observation of a light Higgs particle. As already mentioned, no realistic assessment of the potential of possible future experiments for these measurements is currently available. The issues to be considered include the geometrical acceptance of forward/backward jets and the ability to reconstruct them in presence of large pileup of underlying events as discussed below.

Table 1 [15] summarises the increase in rate for several Higgs production channels in pp collisions, as a function of the beam energy, covering the range of possibilities being considered in this document. Final states with the largest invariant mass (like ttH

[1] $\xi = v^2/f^2$, where $v = 246$ GeV is the EWSB scale, and f is the compositeness scale.

and HH) benefit the most from the energy increase. This benefit is further enhanced when we consider the fraction of events passing the typical analysis cuts imposed to improve signal separation or reduce systematic uncertainties. For example, in the case of ttH production, requiring the top quarks to have a transverse momentum above 500 GeV would increase the rates by a factor of 16 (250) at 33 TeV (100 TeV), instead of the factor of 7 (60) increase for the fully inclusive ttH rate.

In many BSM scenarios for EWSB, the Higgs boson is accompanied by several new particles, with masses in the range of hundred(s) GeV up to possibly several TeV. These could be other Higgs-like scalar states, or heavier partners of the W and Z gauge bosons and of the top and bottom quarks, or, as in the case of supersymmetry, a complete replica of the SM particle spectrum, where each known particle has a partner, with a different spin quantum number. Any deviation of the measured Higgs properties from the SM expectation would imply the existence of at least some of these particles, and viceversa. The mass limits on such new particles derived so far from the LHC still leave ample room for their discovery in the 14 TeV data. However, any discovery at 14 TeV will require a follow-up phase of precision measurements, to understand the origin of the newly observed phenomena. For example, while new Z′ gauge bosons, signalling the existence of new weak interactions, can be discovered with 300 fb^{-1} up to 4–5 TeV, the full HL-LHC luminosity will be needed to determine their properties if their mass is above 2.5 TeV. Existing studies also show that a tenfold increase in the LHC integrated luminosity will extend the discovery reach for new particles by 30–50%.

In the study of the energy frontier with hadron collisions energy and luminosity play a complementary role. Production rates for the signals of interest may be small either because the mass of the produced objects is large or because the coupling strength is small. In the former case, an increase in the beam energy is clearly favourable, while to probe small couplings at smaller masses higher luminosity may be more effective. For a signal at a fixed mass scale M, the cross-section $\sigma(M,g) \propto g^2/M^2 \times L(x=M/\sqrt{S})$ grows with the hadronic centre of mass energy $\sqrt{S}$, since the *partonic* luminosity $L(x)$ grows at least like $\log(1/x)$. An increase in accelerator energy does not need, in this case, to be accompanied by an increase in luminosity. On the other hand, to scale the discovery mass reach M with the beam energy means keeping $x=M/\sqrt{S}$ fixed. In this case the cross-section scales like $\sigma(M,g) \propto g^2/S \times L(x)/x \propto 1/S$ and the collider luminosity must grow as the square of the energy.

Depending on the mass and couplings of these new particles the most effective way to increase their statistics could be either higher luminosity or higher energy. This is illustrated in a simple concrete case in Fig. 1, which represents the LHC discovery potential for new Z′ gauge bosons decaying to lepton pairs, in different energy and integrated luminosity conditions. The reach is expressed by the product of their coupling strength, g, and the square root of the leptonic decay branching fraction. The dashed line corresponds to the result after 3000 fb^{-1} at 14 TeV, the solid blue line to 300 fb^{-1} at 33 TeV. We notice that for masses below ~2.5 TeV the factor of ten higher luminosity at 14 TeV leads to a better discovery reach (or, in the case of a previous discovery, leads to higher statistics and better precision in the measurement of the Z′ properties). On the contrary, if the Z′ is heavier than ~2.5 TeV, the increase in energy is more effective. The figure also shows that the run at 7 TeV has already excluded the existence of Z′ bosons up to 2.5 TeV, at least for some range of their couplings. This means that, at least for some models, a new particle discovered at 14 TeV would be sufficiently heavy that its precision studies would greatly benefit from the energy upgrade, even after the completion of an extensive high luminosity LHC phase. Similar reasoning applies to other BSM new particles. A higher energy pp collider is therefore a powerful tool to extend and improve the precision studies of the Higgs boson and other phenomena to be uncovered during the nominal and high-luminosity LHC runs at 14 TeV, as well as to open the way for the exploration of a new energy range, unattainable by any of the other current proposals for new high-energy facilities.

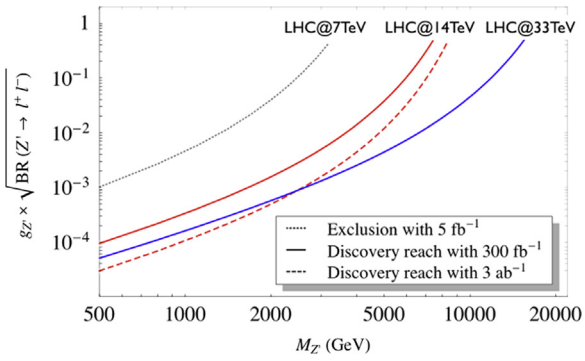

Fig. 1. Discovery potential for new Z′ gauge bosons decaying to lepton pairs, as a function of their mass. The reach is expressed in terms of their coupling strength times the leptonic branching fraction. (For interpretation of the references to color in this figure caption, the reader is referred to the web version of this article.)

The exploration of physics beyond the SM at the high energy frontier will unavoidably require going towards hadron collisions at higher energies. The current limits obtained by LHC at 8 TeV already point in a natural way to higher energies as the best way to perform quantitative studies of possible discoveries made at the LHC at 14 TeV. Even in the absence of such discoveries, the exploratory potential of a high energy pp collider will provide the only opportunity to shed more light on the origin of electroweak symmetry breaking and of the hierarchy problem at the energy frontier.

3. Underlying events in high energy collisions

The large hadronic interaction cross-section at, and above, LHC energies and the intense beam collisions cause the appearance of hadronic activity added to the particles produced in the hard processes of interest. This activity is due to a variety of processes, including initial and final state radiation and multiple parton

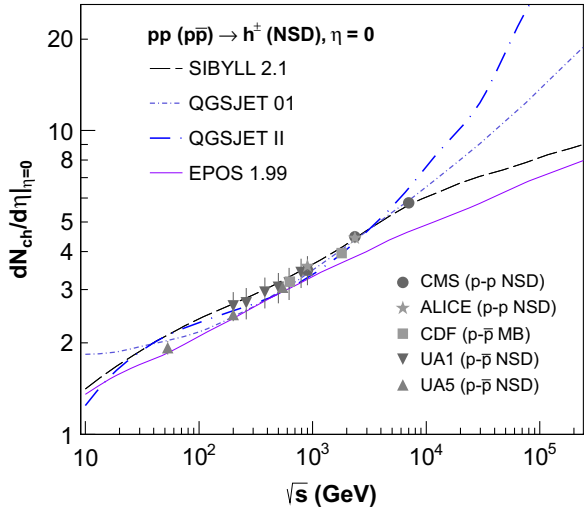

Fig. 2. Scaling of the central charged multiplicity for the SIBYLL, QGSJET, and EPOSmodels compared to collider data for NSD events (from [21], courtesy of the author).

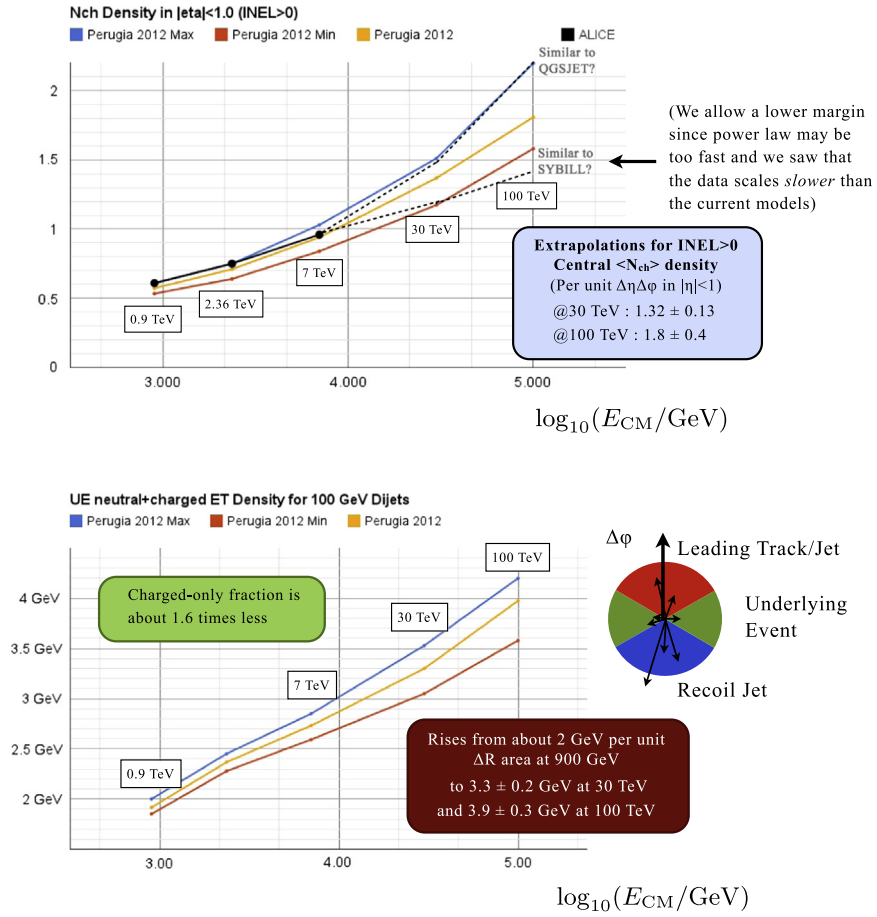

Fig. 3. Extrapolations of the central charged particle density for INEL $>$ 0 events (upper panel), and central UE E_T density for 100-GeV di-jet events (lower panel).

interactions. These underlying events (UE) represent a challenge for experiments at high-luminosity hadron colliders both in terms of detector occupancy and of precision in the reconstruction of the event kinematics. The beam parameters for the LHC high-luminosity upgrade, discussed below, are chosen to mitigate the number of underlying events and keep them within manageable limits for the detectors. Evaluating the rate and characteristics of minimum bias events as a function of the centre-of-mass energy is therefore important for guiding the choice of beam parameters from 14 TeV towards higher energies and assess the experimental conditions [16]. Here, we discuss the rate and characteristics of minimum bias events in collisions above the LHC energy based on the predictions of event simulation programs tuned on the present data.

The total cross-section of minimum bias events can be obtained with a simple Donnachie–Landshoff fit with $\epsilon \sim 0.08$ [17], similarly to the scaling ansätze made in PYTHIA [18,19]. The ALICE measurements of the inelastic and single-diffractive cross-sections [20] do not show any significant deviations from this behaviour over the kinematic range of the measurements. The extrapolations yield an inelastic cross-section growing from $\sim$70 mb at 7 TeV to $\sim$90 mb at 30 TeV and $\sim$105 mb at 100 TeV. The diffractive components increase by only a few mb relative to the LHC values. The underlying events can be characterised in terms of their track multiplicity and associated energy deposition. The extrapolations of central charged track densities in the so-called non-single-diffractive events in pomeron-based models are shown in the left-hand panel of Fig. 2 (from [21]). We estimate the central values and uncertainties by combining the results for various generator tunes, including only those compatible with the scaling observed at the LHC. This yields an estimated central charged-track density per unit of azimuthal angle and pseudo-rapidity, $\Delta R^2 = \Delta\eta\Delta\phi$, of 1.32 ± 0.13 at 30 TeV, and 1.8 ± 0.4 at 100 TeV, for inelastic events with at least one track inside the $|\eta| < 1$ acceptance, which represent $\simeq$85% of all inelastic collisions at 30–100 TeV, compared to about 80% at LHC energies.

A quantity important for the jet energy scale calibrations is the amount of transverse energy deposited in the detector per unit of ΔR^2, and inelastic collision. In the central region of the detector, the Perugia 2012 models [22] are in good agreement with the ATLAS measurements at 7 TeV [23,24], while the activity in the forward region appears to be underestimated [25,23,26,24]. Extrapolations lead to an estimate of (1.25 ± 0.2) GeV of transverse energy deposited per unit of ΔR^2 in the central region of the detector at 30 TeV, growing to (1.9 ± 0.35) GeV at 100 TeV.

The last quantity we consider here is the activity in the underlying events. The most important observable is the summed $p_\perp$ density in the so-called "transverse" region, defined as the wedge 60–120° away in azimuth from a hard trigger jet. For $p_\perp^{\text{jet}}$ values above 5–10 GeV, this distribution is effectively flat, i.e. to first approximation it is independent of the jet $p_\perp$. It does, however, depend significantly on the centre-of-mass energy of the pp collision, a feature which places strong constraints on the scaling of the $p_{\perp 0}$ scale of MPI models. Given the good agreement between the Perugia 2012 models and the Tevatron and LHC UE measurements [24], we estimate the E_T (neutral+charged) density in the transverse region (inside $|\eta| < 2.5$), for a reference case of 100 GeV di-jets in the bottom pane of Fig. 3. Starting from an average of about 2 GeV per unit of ΔR^2 at 900 GeV, the density rises to (3.3 ± 0.2) GeV at 30 TeV and to (3.9 ± 0.3) GeV at 100 TeV, while the charged-only fraction should be lower by a factor $\sim$1.6. These predictions show that the underlying event activity at energies above that of the LHC does not appear to represent a major obstacle for exploiting the physics potential of high energy hadron colliders.

4. LHC luminosity upgrade

The full exploitation of the LHC is the highest priority of the energy frontier collider program. LHC is expected to restart in Spring 2015 at centre-of-mass energy of 13–14 TeV and to reach the design luminosity of 10^{34} $cm^{-2}\,s^{-1}$ during 2015. This peak value should give a total integrated luminosity over one year of about 40 fb^{-1}. In the period 2015–2020, the LHC will gradually increase its peak luminosity. Margins have been taken in the design to allow the machine to reach about two times the nominal design performance. The baseline program for the next decade is schematically shown in Fig. 4 with the expected evolution of the peak and integrated luminosity.

The LHC has so far provided collisions at 8 TeV centre-of-mass energy with total beam currents of about 0.4 A (i.e. 70% of the nominal design value but with only half the nominal number of bunches). Once the magnet interconnections are consolidated and the beam energy limits removed, as well as some radiation-to-electronic (R2E) intensity limits mitigated during current LS1 phase, the design luminosity will hopefully be attained and possibly exceeded. Then, by removing the outstanding beam intensity limits in the injector chain and the LHC during additional shutdowns following the LS1, the LHC will head toward the so-called *ultimate* design luminosity, which is about twice the nominal luminosity, i.e., 2×10^{34} $cm^{-2}\,s^{-1}$. This ultimate luminosity performance was planned to be reached by increasing the bunch population from 1.15 to 1.7×10^{11} protons, with a bunch spacing of 25 ns (beam current increases from 0.58 A to 0.86 A). Transforming this ultimate peak performance into a doubling of the annual integrated luminosity will however be very difficult and it is more likely that the delivered luminosity will be around 60–70 fb^{-1}/year.

After 2020 some critical components of the accelerator will reach the radiation damage limit and others will see their reliability reduced because of vulnerability to radiation, wear and high intensity beam operation. Therefore, important consolidation actions are required before 2020, just to keep the LHC running with a good availability. Further, the statistical gain in running the accelerator without an additional considerable luminosity increase beyond its design value will become marginal, therefore the LHC will require to have a decisive boost of its luminosity.

This new phase of the LHC life, named High Luminosity LHC (HL-LHC), has the scope of preparing the machine to attain the threshold of 3000 fb^{-1} of integrated luminosity during 10–12 years of operation. The project is now the first priority of Europe, as stated by the Strategy update for High Energy Physics group approved by CERN Council in a special session held on 30 May 2013 in Brussels.

4.1. HL-LHC

The LHC pp nominal design luminosity for each of the two general purpose experiments (ATLAS and CMS) is $L_0=10^{34}$ $cm^{-2}\,s^{-1}$. This luminosity is associated with a bunch spacing of 25 ns (2808 bunches per beam) and gives an average value of 27 underlying events/crossing. The main objectives of HL-LHC are the following:

1. peak luminosity of 5×10^{34} $cm^{-2}\,s^{-1}$ with levelling,
2. integrated luminosity of 250 fb^{-1}/year, enabling the goal of 3000 fb^{-1} within twelve years after the upgrade.

This luminosity is about ten times the luminosity reach of the first twelve years of the LHC lifetime. The luminosity upgrade provides the collider particle physics community with an unprecedented data sample taken at the frontier constituent energy, which will be key to investigate the dynamic of EWSB and answer some of the most important open questions in particle physics discussed above.

The HL-LHC project is matched by a companion LHC detector upgrade program, to ensure that the detectors will keep their outstanding performance while operating with an average of ~140 underlying events. The 5×10^{34} $cm^{-2}\,s^{-1}$ value for the luminosity levelling corresponds to the nominal 25 ns bunch spacing. For a 50 ns bunch spacing, the levelling value would be half of this value with the unavoidable loss of integrated luminosity. The experiments are actually designing their upgraded detectors to be capable of sustaining an average of 140 events/crossing and a maximum of 190–200, thus keeping a reasonable margin against shortfalls, including a possible run of the machine at 50 ns should 25 ns become too difficult, and pile-up fluctuations around the average rate [7].

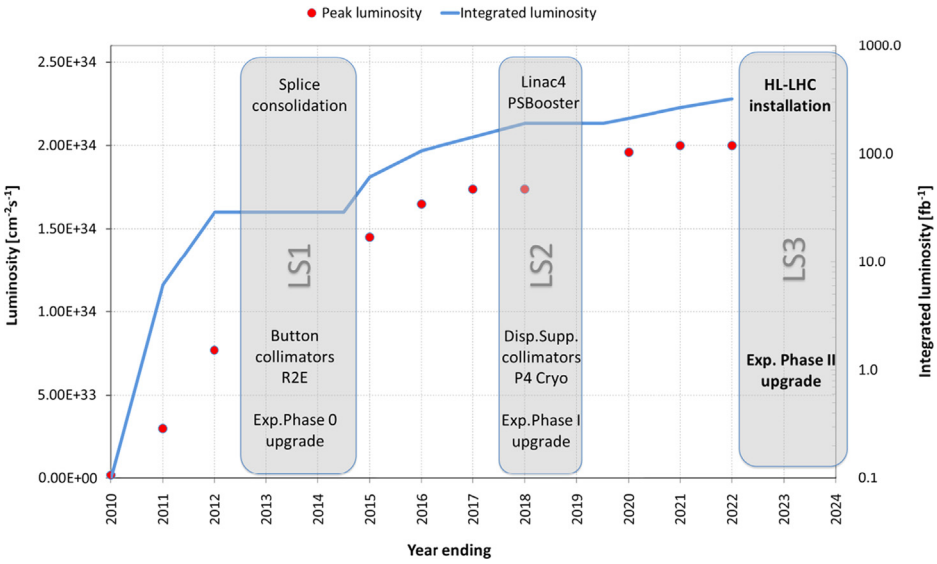

Fig. 4. LHC baseline plan for the next decade. The current long shutdown (LS) 2013–14 is to allow design parameters of beam energy and luminosity. The second LS, scheduled mid-2018–2019, is to increase the beam intensity and reliability as well as to upgrade the LHC injectors. A forecast of the peak and integrated luminosity is also given.

4.2. Beam parameters

Experience with the LHC shows that the best set of parameters for actual operation is difficult to predict, before we obtain operational experience with the 7 TeV beams. The upgrade studies should therefore provide the required HL-LHC performance over a wide range of parameters, and the machine and experiments will find the best set of parameters during operation, once the LHC runs at the maximum energy and with above nominal beam intensities.

The (instantaneous) luminosity L can be expressed as

$$L=\gamma\frac{n_b N^2 f_{rev}}{4\pi\beta^*\epsilon_n}R, \quad R=\frac{1}{\sqrt{1+\frac{\theta_c\sigma_z}{2\sigma}}} \tag{1}$$

where γ is the proton beam energy in unit of rest mass, n_b is the number of bunches in the machine: 1380 for 50 ns spacing and 2808 for 25 ns, N is the bunch population. $N_{nominal,25\ \mathrm{ns}}=1.15\times 10^{11}$ p ($\rightarrow$0.58 A of beam current at 2808 bunches), f_{rev} is the revolution frequency (11.2 kHz), β^* is the beam beta function (focal length) at the collision point (nominal design 0.55 m), ϵ_n is the transverse normalised emittance (nominal design: 3.75 μm), R is a luminosity geometrical reduction factor (0.85 at 0.55 m of β^*, down to 0.5 at 0.25 m), θ_c is the full crossing angle between colliding beam (285 μrad as nominal design), σ, σ_z are the transverse and longitudinal r.m.s. size, respectively (16.7 μm and 7.55 cm). Table 2 lists the main parameters of the scenarios considered here. The parameters for the HL-LHC [8,3] are given in the third column. The 25 ns bunch spacing is the nominal operating target. However, a scheme with 50 ns is also being considered, as fall-back solution. In order to reach the goal of 250 fb^{-1}/year with 160 days dedicated to proton physics, the efficiency must be $\geq$60%. A big leap forward is required by increasing the availability and reducing the turnaround time, i.e. the time from end of physics to next start of physics.

The nominal total beam current of 1.12 A (see Table 2) is a difficult target to attain. It represents a hard limit for the LHC since it affects many systems, such as RF power systems and RF cavities, collimation, cryogenics, kicker magnets, vacuum system, beam diagnostics, in a direct way, and several others, like quench detection system of the SC magnets and virtually all controllers, in an indirect way, due to an increase of the R2E events. Transverse emittance is assumed to be very low also in view of the already better than the design value results during the first LHC run. However, getting the beam brightness, N_p/ϵ_n, required for HL-LHC is a very difficult challenge for the injector chain, even after upgrades, as well as preserving it in the LHC.

In view of these limitations, the classical route available to increase the luminosity is the reduction of the beam focal length at the IP, β^*, by means of triplet magnets which have larger aperture for a given gradient or are longer and larger aperture low-β triplet quadrupoles with a reduced gradient. A reduction in the β^* value implies an increase of beam sizes over the whole matching section. Therefore the reduction in β^* implies not only larger triplet magnets but also larger separation/recombination dipoles and larger and/or modified matching section quadrupoles. A previous study showed that a practical limit in the LHC arises around $\beta^*=30$–40 cm. However, a recently proposed scheme, the Achromatic Telescopic Squeeze (ATS) [27], would allow to enhance the beam squeezing capability of the low-β triplet magnets and overcome these limitations in the LHC matching section. Thanks to the adoption of Nb_3Sn quadrupoles of larger aperture and higher field, a β^* value of 15 cm or even 10 cm can now be envisaged and flat optics with a β^* as low as 5 cm in the plane perpendicular to the crossing plane are possible. In particular, a value of $\beta^*=10$ cm has recently been attained in an LHC machine development run dedicated to test the ATS principle. This progress offers margin compared to the parameters given in Table 2.

In order to be compatible with such small β^* values, the aperture of the low-β^* quadrupole magnets needs to be doubled, which causes a peak field 50% higher than that of the present LHC triplet magnets and requires a new superconducting magnet technology based on Nb_3Sn, as discussed in the next section. The drawback of the very small β^* values is that they require a larger crossing angle, which entails in turn a reduction of the luminosity via the geometrical factor of beam overlap, R, defined in Eq. (1), compared to the LHC present conditions (see Fig. 5). The reduction of the beam separation at the parasitic encounters and the mitigation of the beam-beam effects are under study but not yet

Table 2
Parameters of LHC, HL-LHC, HE-LHC, and FCC-hh. The luminosity given for HL-LHC assumes the use of crab cavities.

Parameter	LHC	HL-LHC [8,3]	HE-LHC [4]	FCC-hh [5]
c.m. energy (TeV)	14	14	33	100
Circumference C (km)	26.7	26.7	26.7	80
Dipole field (T)	8.33	8.33	20	20
Dipole coil aperture (mm)	56	56	40	$\leq$40
Beam half aperture (cm)	$\sim$2	$\sim$2	1.3	$\leq$1.3
Injection energy (TeV)	0.45	0.45	$>$ 1.0	$>$ 3.0
No. of bunches n_b	2808	2808	2808	8420
Bunch population N_b (10^{11})	1.15	2.2	0.94	0.97
Init. transv. norm. emit. (μm)	3.75	2.5	1.38	2.15
Initial longitudinal emit. (eVs)	2.5	2.5	3.8	13.5
No. IPs contributing to tune shift	3	2	2	2
Max. total beam-beam tune shift	0.01	0.015	0.01	0.01
Beam circulating current (A)	0.584	1.12	0.478	0.492
rms bunch length (cm)	7.55	7.55	7.55	7.55
IP beta function (m)	0.55	0.15 min	0.35	1.1
rms IP spot size (μm)	16.7	7.1 min	5.2	6.7
Full crossing angle (μrad)	285	590	185	72
Stored beam energy (MJ)	362	694	701	6610
SR power per ring (kW)	3.6	7.3	96.2	2900
Arc SR heat load (W/m/aperture)	0.17	0.33	4.35	43.3
Energy loss per turn (keV)	6.7	6.7	201	5857
Critical photon energy (eV)	44	44	575	5474
Photon flux (10^{17}/m/s)	1.0	2.0	1.9	2.0
Longit. SR emit. damping time (h)	12.9	12.9	1.0	0.32
Horiz. SR emit. damping time (h)	25.8	25.8	2.0	0.64
Init. longit. IBS emit. rise time (h)	57	23.3	40	396
Init. horiz. IBS emit. rise time (h)	103	10.4	20	157
Peak events per crossing	27	135 (lev.)	147	171
Total/inelastic cross-section (mb)		111 / 85	129 / 93	153 / 108
Peak luminosity (10^{34} cm^{-2} s^{-1})	1.0	5.0	5.0	5.0
Beam lifetime due to burn off (h)	45	15.4	5.7	14.8
Optimum run time (h)	15.2	10.2	5.8	10.7
Opt. av. int. luminosity/day (fb^{-1})	0.47	2.8	1.4	2.1

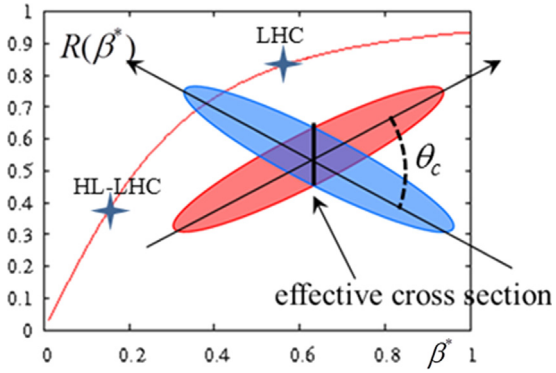

Fig. 5. Geometrical reduction factor of luminosity, R, vs. β^* with the two operating points for the nominal LHC and HL-LHC beam parameters indicated by the crosses.

fully demonstrated. In the HL-LHC design, the reduction in the geometrical factor R is compensated with the use of crab cavities, which rotate the beams before collisions to maximise their overlap [28,29]. Their development is discussed in the next section.

5. Technology aspects

The energy reach of hadron colliders is largely dictated by the length of the tunnel and the performance characteristics of the magnet technology. The beam energy, E, is directly proportional to the magnetic dipole field strength, B, and the tunnel radius R, according to the well-known relation $E = 0.3B\,(\mathrm{T}) \times R\,(\mathrm{km})$, which implies a direct tradeoff between the cost of the tunnel, $\propto R$, and that of the magnet system. Magnet costs typically grow proportionally to field strength B, except when operated close to the conductor critical field and with significant step increases associated with the use of more advanced conductors. Tunnel limitations are related to a variety of issues, ranging from rock and soil conditions, terrain profile and costs and are strongly site dependent. The magnet systems for major colliders consist primarily of superconducting dipoles and quadrupoles, which provide the requisite beam guidance and focusing, respectively. These systems, together with tunnel/facilities, are the cost drivers for a collider. The magnet systems are also a major technical challenge, requiring expertise in materials, design, analysis and fabrication processes to bring the technology to a state of readiness for application to large accelerator projects.

Superconducting dipoles have formed the backbone of all major hadron colliders in the last couple of decades, including the Tevatron, HERA, RHIC and now the LHC. The present LHC is based on ~40 years of development in the domain of superconducting (SC) magnet technologies [30,31]. Its NbTi-based magnets are pushed to their limits; the very compact two-in-one magnets provide 8.3 T of operating field by using superfluid helium cooling.

We note that the infrastructure and expertise needed to make significant progress in this field are the result of long-term vision and support from HEP funding agencies [32]. The developments that have occurred in high-field dipole magnet performance over the last two decades, shown in Fig. 6, have been made possible by the availability of adequate resources. The dipole field strengths obtained through dedicated R&D programs enable the community to consider collider configurations with energies significantly beyond the LHC, as shown in Fig. 7. Based on the developments to date, we can make some general assessment on the current

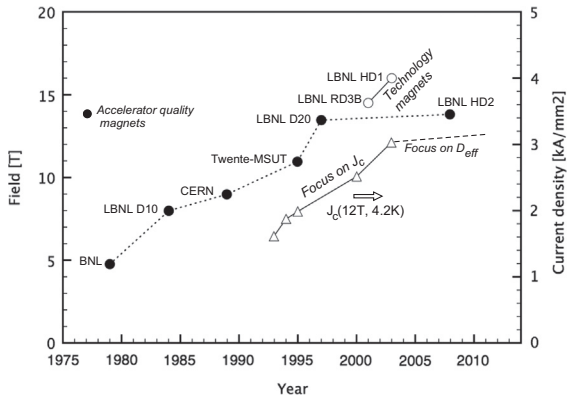

Fig. 6. Progress in superconducting dipole magnet performance and increase in J_c(12 T, 4.2 K) of Nb_3Sn over the last 20+ years. The RD3 and HD1 refer to simple race track prototypes for technology tests.

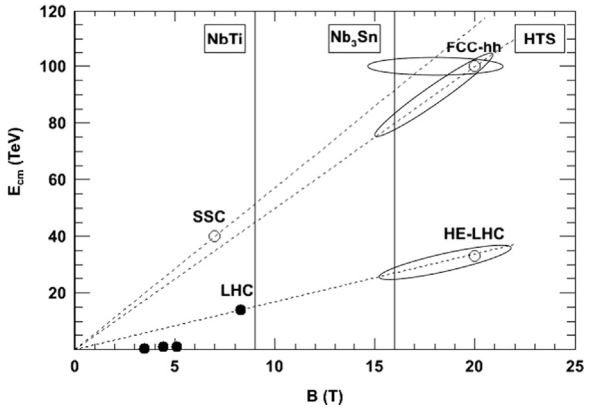

Fig. 7. Role of the superconductor in the energy reach of hadron colliders as a function of magnet field and accelerator radius. The ellipses show the tradeoff in attainable energy and ring radius associated with the use of HTS materials compared to Nb_3Sn.

status and potential future of magnet development: The technology basis (conductor, engineering materials, and mechanical structures) for dipole magnets generating ~14–16 T fields is now becoming available. This is not to say that the technology is ready for implementation: only short prototypes have yielded fields in this range, and without operating margin. The prototypes do, however, demonstrate that forces and stresses associated with these fields can be supported and managed. The margin can be obtained at the expense of larger magnet size and more conductor. Furthermore, the required margin should be minimised by thorough understanding and control of the design and fabrication of the magnets. To bring this technology to a state of readiness for application in a future collider will require a focused technology readiness effort, similar to that of LARP and of a similar timescale (~10 years) and funding level.

On the other hand, the technology basis for 20+ T dipoles is not yet in place. Work in this area is ongoing on multiple fronts, including development of conductor and cables, engineering materials, and mechanical structures. Strong R&D support for these efforts, similar to that provided to the magnet research groups over the last decade, can be expected to yield first prototype results within a ~5 year time frame. If these developments are successful, a follow-on phase of technology readiness should be again envisioned, in order to bring this technology to the state needed for its implementation in an accelerator project. For these magnets, the conductor developments are critical, and magnet support must be matched with appropriate support for conductor R&D.

The dipole magnet R&D is well-leveraged, in the sense that it serves both hadron and muon colliders. We note that in addition to field strength, magnet programs need to take into consideration cost-effectiveness and scalability in magnet designs. As noted earlier, the superconducting dipoles for a future collider will dominate the facility cost. Furthermore, they are technically one of the highest-risk components. Designs must be adequate for industrialisation to leverage the strength of the private sector in providing cost-effective fabrication during mass production.

The HL-LHC upgrade program requires quadrupoles with peak field in excess of 12 T, and heavily relies on the success of the advanced Nb_3Sn technology, developed initially by the US magnet programs and refined and matured by LARP, since the NbTi superconductor used in the present LHC magnets is limited to field strengths below 8–9 T [33–35]. Besides magnets, many other technologies are involved, like crab cavities, advanced collimators, SC links, advanced remote handling, etc. The HL-LHC is a medium size project and implies deep changes and new installations over

about 1.2 km of the LHC ring. Beside addressing its physics goals, the HL-LHC will pave the way to a larger project like a higher energy LHC, which is based on a further enhancement of the same technologies. In fact, the technological development of high-field magnets and other components discussed below, which are key to the HL-LHC program, connect the mid-term upgrade path of the LHC to the long-term developments towards hadron colliders of even higher energy. These programs have also important overlaps with other HEP research areas, such as muon acceleration and accelerators for the intensity frontier, in the fields of magnet and collimation systems.

In summary, it is important to continue a focused integrated program emphasising engineering readiness of technologies suitable for high energy hadron colliders and with applications to other accelerator programs. In this section, we discuss the technological aspects of high field magnets from the conductor development to specific designs, the HL-LHC collimation issues and the crab cavity R&D.

5.1. Conductor development for SC magnets

Superconductor properties form the basis of magnet performance. The main low-temperature superconductors (LTS) used in accelerator magnets are NbTi and Nb_3Sn. All SC magnets for colliders to-date have been based on a LTS material, NbTi, which has a critical field $B_{c2} \approx 13.7$ T at 1.8 K. NbTi-based accelerator technology has been pushed to its limit in the development of the LHC dipoles, with operating fields of 8.3 T at 1.9 K. Accelerator magnet research since then has focused for the most part on another low-temperature superconductor, Nb_3Sn, which has a much higher critical field, $B_{c2} \approx 27$ T at 1.8 K (see Fig. 8), and which can provide access to fields beyond the intrinsic limitation of NbTi technology [36]. Nb_3Sn is a brittle inter-metallic compound, which imposes significant constraints on the design, fabrication and implementation of the material in accelerator magnets.

A number of properties are of importance for accelerator applications. First, the field-temperature phase-boundary, defined by the behaviour of the current density, $J_c(B,T)$, dictates both the efficiency of field production and the maximum attainable field strength. Second, the superconducting filaments have a characteristic size D_{eff} which must be small enough to minimise the amplitude and influence of persistent currents. For accelerator dipole application $D_{eff} \sim 20$ μm (or less) is desirable. A sufficient high-quality stabiliser, typically Cu, must be provided to allow the conductor to recover from transient thermal events such as small scale epoxy cracking, motion, or flux-jump events. This is usually specified in terms of the Cu fraction and in terms of the residual resistivity ratio, RRR. The filament size D_{eff} can also impact stability, further motivating small filaments. Finally, the conductor industrial production must be capable of maintaining dimensions and metallurgical properties over lengths commensurate with the magnet needs. For Nb_3Sn, improvements in all of these properties have been the focus of the DOE-funded Conductor Development Program (CDP), initiated in 1999, which provides funds for the support of industrial improvements that are focused on specific target areas [38]. Over the last ~15 years, the industry has made tremendous progress in Nb_3Sn. The current-density figure of merit $J_c(12\,\mathrm{T}, 4.2\,\mathrm{K})$ has tripled to $J_c(12\,\mathrm{T}, 4.2\,\mathrm{K}) > 3000\ \mathrm{A/mm^2}$. Ongoing efforts focus on reducing the filament characteristic size, D_{eff}, by increasing the number of filaments in the wire, and in improving the residual resistivity ratio, RRR, through improvements in the barrier surrounding the filaments.

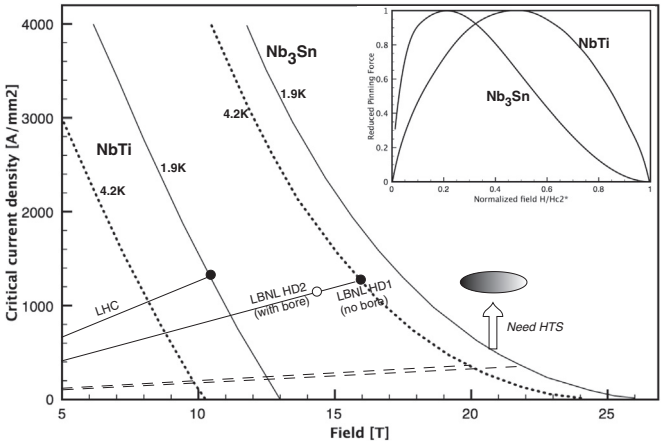

Fig. 8. Critical current of NbTi and Nb_3Sn at 1.9 K and 4.2 K, respectively. The inset shows the corresponding normalised pinning force for each conductor. Load-lines for the LHC NbTi dipoles and the LBNL Nb_3Sn high-field dipole model magnets HD1 (without bore) and HD2 (with bore) are also given (modified from [37]).

A fairly new area of conductor development pertains to high-temperature superconductors (HTS). The HTS materials, primarily $Bi_2Sr_2CaCu_2O_x$ (Bi–2212) and $YBa_2Cu_3O_{7-\delta}$ (YBCO), are under investigation for a high-field magnet applications. At low-temperatures (e.g. 1.8-4.5 K) these materials exhibit good current densities at high magnetic fields. In fact, $J_c(B)$ is nearly independent of the field value, above ~10 T. These materials are very different in nature. The YBCO is effectively a 1–4 μm-thick single-crystal sheet deposited on a substrate material. Once fabricated it is superconducting upon cool down to cryogenic temperatures. The superconductor is characterised by a strong anisotropy in its $J_c(\vec{B})$ dependence. Use of YBCO is further complicated by the form of tape, which makes difficult to assemble various units in a compact large cable, capable to carry current of 10 kA as required for accelerators magnets. However, YBCO has also some strong points, such as its good mechanical strength (important for high field, high stress magnets), critical current improving with the R&D and it has become a reference material attracting considerable effort, given the promise of important cost reduction after industrialisation.

Bi-2212 is fabricated using Bi–Sr–Ca–Cu oxide powder imbedded in a silver tube. This is then processed into a wire using the basic processing of LTS materials. The resulting wire must undergo a high-temperature (~900 °C) treatment in pure oxygen environment in order to generate the Bi-2212 superconductor. The result is an isotropic conductor characterised by superconducting grains aligned along the wire axis. Over the last few years collaborative work has aimed at developing Bi-2212 as a viable conductor for magnet applications, together with industry. This work has demonstrated that the wire could be cabled into the standard Rutherford cable configuration for a current-scalable conductor. Groups proceeded to design, fabricate and test the first solenoid and racetrack coils [39,40]. This effort demonstrated the basic viability of the conductor. However, it made clear that the effective ("engineering") current density (J_E) of the wire was not suitable for accelerator magnet application. Effort on Bi-2212 was successful in demonstrating that the J_E could be tripled, by modifying the processing to include high-pressure during the heat treatment, thereby dramatically reducing porosity in the final conductor [41,42]. This development is now the focus of renewed interest by the magnet community, with active programs in place to demonstrate dipole and solenoid inserts for accelerator applications [43].

5.2. High field magnets for HL-LHC

The progress in magnet performance over the years from the resistive magnet era through the jump in performance required by

HL-LHC and the development towards a higher energy machine, is summarised in Fig. 9.

However, field strength alone is not sufficient [44]. Radiation escaping from the collision point through the beam pipe has two main effects: (i) heat deposition that may limit the performance of the SC magnets by increasing the conductor temperature; (ii) radiation damage, especially to insulation but also to metallic components. Radiation damage for magnets exposed to the radiation near the experiments is directly proportional to the integrated luminosity and might occur around an integrated luminosity of 300 fb^{-1}, which is probably a conservative estimate. Heat deposition may limit the peak luminosity at about 1.7–2.5 $\times$ 10^{34} cm^{-2} s^{-1}. In both cases this means that sometime after 2020 we need to change the low-β quadrupole triplets. This is a unique chance to replace them with magnets of new generation, capable of higher performance and making the full system more robust against radiation and other factors which would otherwise reduce the availability of the machine. In addition to the replacement of the quadrupole, the whole Interaction Region (IR) zone needs to be redesigned with larger aperture recombination/separation dipole magnets (D1/D2 pair), new distribution feed-boxes (DFBX), cryo-distribution electrical feed-box of the low-β triplet and improved access to various equipment for maintenance. The cryogenic system will also need to be improved and the power supplies and distributed feed-back (DFB) most critical in terms of radiation exposure should be placed out of the tunnel. Power supplies and DFB would be relocated on ground, by means of powerful 150 kA SC links, to reduce the time of intervention and make maintenance easier. Many other systems, such as SC magnet protection, interlock, etc., will also need to be upgraded to improve the machine availability, essential to achieve high integrated luminosities, as mentioned above.

Today high-field accelerator prototype magnets, including the LARP quadrupoles, use conductors with a current density of $J_c(12\,T, 4.2\,K) \simeq$ 2500–3000 A/mm^2, approximately 3 times larger than that used in the magnets for the ITER fusion program. This has been possible thanks, in part, to the long-term CDP run by DOE-HEP. As conductor transport current improves, magnet field progresses in-step, as shown by the progress of the maximum field in short Nb_3Sn dipole or quadrupole magnets (what we call models, typically 1 m long or less). Nb_3Sn magnet record field performance are obtained after many quenches and in conditions far from operation in an accelerator. Still, the performance required at the HL-LHC is now within reach. The LARP quadrupoles have reached the 12 T field level on the conductor with an aperture of 90–120 mm, much larger than that of the present LHC quadrupoles (56–70 mm) and already very close to the 150 mm aperture which is the target value for the HL-LHC. In Fig. 10 the new triplet scheme for the HL-LHC upgrade is shown. Special tungsten shielding will be placed inside inner bore to limit the radiation deposition to the same level of the nominal LHC, about 30 MGy, despite the ten time higher integrated luminosity.

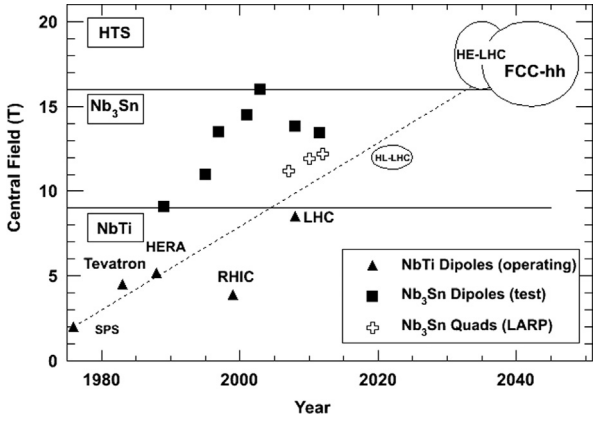

Fig. 9. Progress of accelerator magnets for hadron colliders. Below 9 T, the realm of Nb–Ti, the figure gives the nominal operating condition of Nb–Ti magnets used in the present machines. Beyond 9 T, where Nb_3Sn is needed, the results for prototype magnets and record field achieved are shown. The results included here are for magnets with different apertures. Early Nb_3Sn dipoles have 50 mm bore while the newer prototypes feature an aperture of 40 mm, except for the two technology test magnets delivering the highest field at 14 and 16 T, which are racetrack coils with no bore. The HD series features an aperture of 40 mm. LARP quadrupoles have 90 (LQ) or 120 (HQ) mm apertures. For comparison, HL-LHC requires a 150 mm quadrupole aperture.

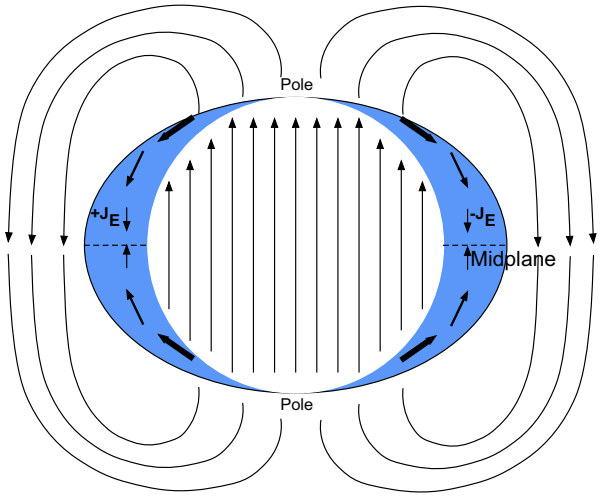

Fig. 11. Schematic of a $\mathrm{Cos}(\theta)$ current density distribution and azimuthal forces. Note that the forces accumulate on the azimuth, resulting in peak stress on the mid plane of a $\mathrm{Cos}(\theta)$ dipole.

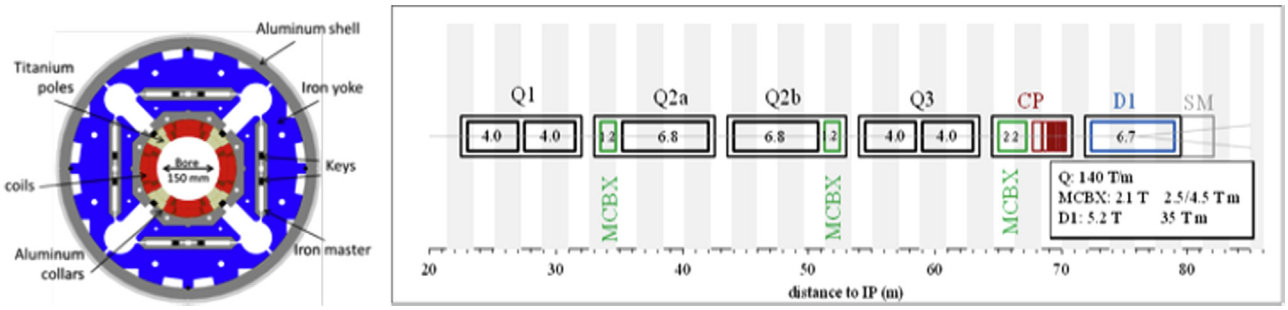

Fig. 10. Cross-section of the 150 mm aperture quadrupole of the inner triplet under development by CERN and the US LARP program (left panel). Layout of the HL-LHC IR (inner triplet, correctors and D1) (right panel).

5.3. High field magnet R&D for pp colliders beyond the LHC

In order to understand the issues driving high-field dipole development, it is helpful to consider here the fundamental design limitations. The concept of a $\mathrm{Cos}(\theta)$ dipole is shown in Fig. 11. The field produced by a perfect $\mathrm{Cos}(\theta)$ current density distribution is a function of the current density J_E and coil width w, and independent of the radius r as shown in Fig. 12. Hence the volume of conductor (V) needed to produce a field B_0 scales with bore size. Inside the coil, the field magnitude decreases with radius; since the conductor can carry more current at lower field, designs can "grade" the conductor, i.e. use smaller conductors in the lower field regions, to produce the same field more efficiently (i.e. with less overall conductor). Implementing grading in a high field $\mathrm{Cos}(\theta)$ dipole results in dramatic increase in $\sigma_{\theta m}$, since w decreases and J_E increases with r when grading is incorporated.

The Lorentz force $F_\theta \sim J_E B_r$ accumulates along the azimuth, resulting in maximum stress $\sigma_{\theta m}$ on the midplane (see Fig. 11). Experience with Nb_3Sn magnets has lead to well-established limitations $\sigma_{\theta m} < 200$ MPa on the compressive mid plane stress. Beyond this value the conductor degrades and magnet performance becomes unreliable. Due to the accumulation, stress on a $\mathrm{Cos}(\theta)$ coil of radius r and thickness w scales as

$$\sigma_{\theta m} \propto r J_E / w. \tag{2}$$

Fig. 13 provides an example for a Nb_3Sn ~18 T coil layout (with no operating margins). It is important to note that the graded scenario far exceeds the stress limitation for the material.

Stress is a dominant limitation for high-field dipole designs. From Eq. (2) it is evident that $\sigma_{\theta m}$ can be reduced to acceptable values by reducing the current density and making the coil cross-section larger. This comes at the expense of significant more conductor to be used. Furthermore, the actual stress state in the $\mathrm{Cos}(\theta)$ design is an even more complex phenomenon than described above, due to significant radial forces acting on the coils, predominantly in the midplane region. The importance of stress accumulation in dipole magnets has been recognised for some time. Alternative magnet designs, using "block" coils in various configurations, has been the focus of much effort over the last ~15 years. A concept of stress management was proposed by the Texas A&M group [45]. The idea is to intercept stress before it can accumulate to unacceptable values. An alternative approach, using a "canted $\mathrm{Cos}(\theta)$" design concept [46] shown in Figs. 14 and 15, is currently under investigation at LBNL.

A hybrid block-dipole magnet has been developed by the CERN group, which allows for grading of the conductor, and includes YBCO coils in the high-field region, Nb_3Sn in the "middle" field region, and NbTi in the low-field region, The magnet design aims at 20 T operating field (i.e. with a ~20% margin over its maximum theoretical field) (see Fig. 16). The design builds on the experience from the LBNL HD-series of block dipoles and the CERN Fresca2 design.

5.3.1. Magnet protection

Another important limitation of high-field dipoles and quadrupoles relates to the stored magnetic energy E_m. The stored

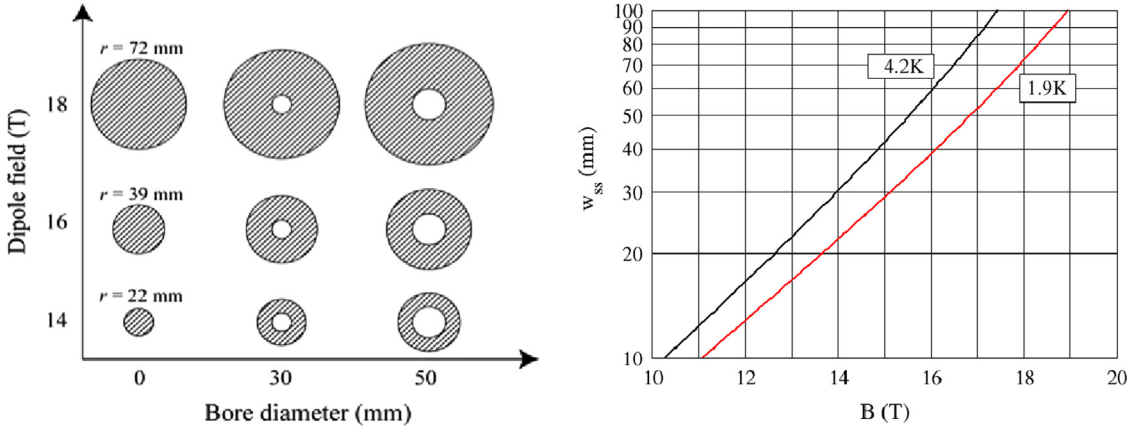

Fig. 12. Field produced by a $\mathrm{Cos}(\theta)$ current density distribution, which is a function of coil width and current density, but not of the coil radius. The right panel shows the coil width required to generate a given central field, based on state-of-the-art modern conductor yielding J_c(12 T, 4.2 K)=3000 A/mm^2.

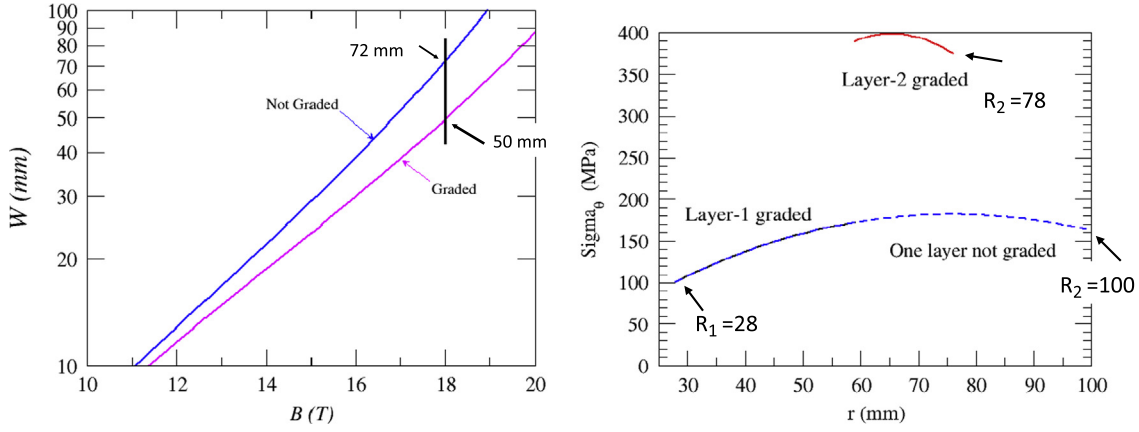

Fig. 13. Improvement in field-generating efficiency of $\mathrm{Cos}(\theta)$ current density distribution using "grading" (left panel). Enhancement of $\sigma_{\theta m}$ associated with grading of a $\mathrm{Cos}(\theta)$ magnet (right panel). Values correspond to those of a ~18 T Nb_3Sn magnet.

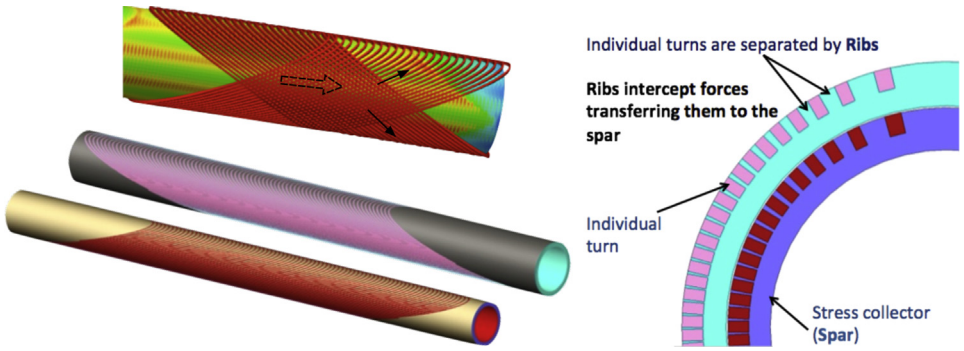

Fig. 14. Concept of a canted $\mathrm{Cos}(\theta)$ magnet. The current in each layer produces solenoidal and dipole field components. Layers are assembled one inside another and, from one layer to the next, the solenoidal field cancels. The effective current distribution closely approximates a perfect $\mathrm{Cos}(\theta)$ distribution. Azimuthal forces acting on each cable are captured by the ribs. Radial forces are intercepted by the spars and supported via pre-stress from the external structure. Peak stresses on the conductor are significantly lower than for existing high-field dipoles, reduced by an order of magnitude compared to an equivalent $\mathrm{Cos}(\theta)$ design.

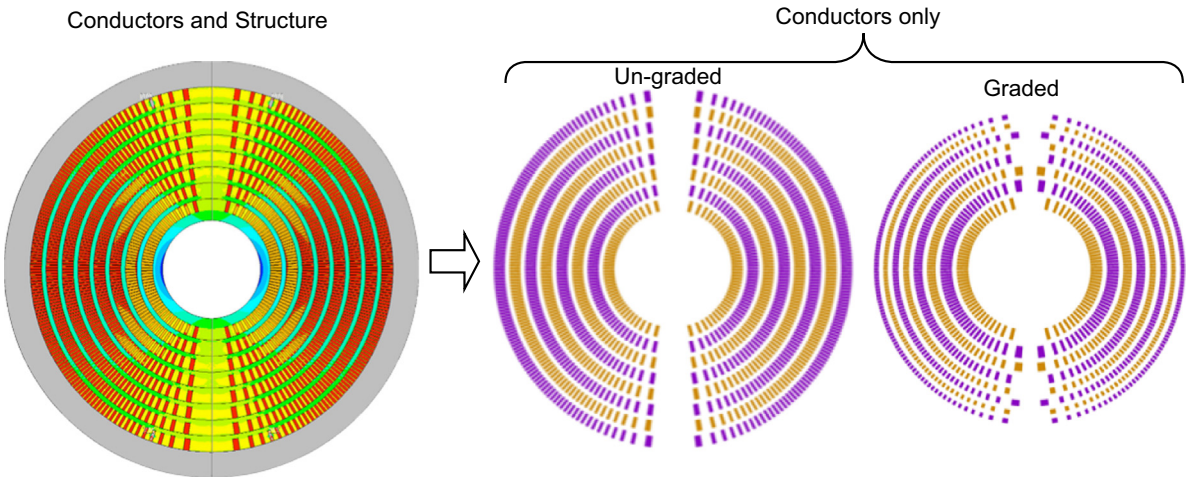

Fig. 15. Layout of a 100-mm bore canted $\mathrm{Cos}(\theta)$ magnet with 8 layers, corresponding to a $\sim$16 T design. The left panel shows the complete cross-section including spars, ribs, and conductors as in Fig. 14. The value of grading with Nb_3Sn is shown in on the right panel. The cross-sections show conductors only, for un-graded and graded designs. Note the significant reduction in size of the graded magnet. The two designs yield the same central field, with the graded magnet requiring 40% less conductor compared to the un-graded design.

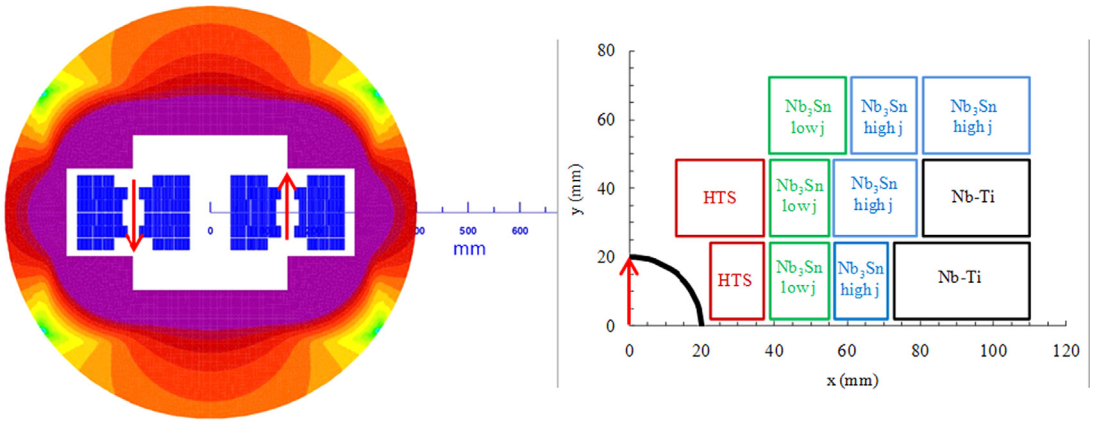

Fig. 16. Concept of a hybrid block-dipole 2-in-1 magnet yielding 20 T [47]. The design uses YBCO coils in the high-field region, Nb_3Sn in the "middle" field region, and NbTi in the low-field region. The design meets basic requirement of field quality and mechanical stress. More detailed evaluation of many aspects, including construction technique, peak stresses and magnet protection, are underway.

magnetic energies $E_m \propto \pi r^2 B_0^2 L$, where L is the magnet length, results in significant heating of the magnet in the case of a quench, i.e. the sudden irreversible loss of superconductivity at some point in the conductor. Highly specialised magnet protection circuitry is now employed in high-field accelerator magnets, typically incorporating the following features:

- fast detection of a quench onsite, typically within a few milliseconds of quench initiation - the detection must discriminate between real quench signals and false triggers emanating from flux jumps that can randomly occur;
- firing of heaters distributed in the magnet to force a large fraction of the superconductor into the normal (non-superconducting)

state and to force the drive current to flow in a parallel bus bar line;
- activation of an external dump resistor to extract a significant fraction of the power away from the magnet and to protect the parallel bus bar line.

All of these events must happen on a timescale of $\mathcal{O}$ (10 ms) in order to prevent areas of the magnet from overheating. As the current densities in superconductors improve and higher-field magnets with larger bore are developed, magnet protection becomes an increasingly significant technical challenge.

5.3.2. Field quality

Dipole magnets for a future collider will have strict requirements on multipole content and hysteresis. These issues are impacted by the choice and characteristics of the superconductor and by the magnet design. SC wires are composed of a large number of filaments that are then twisted to minimise coupling losses, i.e. resistive Joule heating generated by dB/dt during magnet ramping. The filaments themselves can support persistent currents that impact field quality and are hysteretic in nature. Furthermore, the filaments can experience sudden flux-penetration ("flux-jumps") as fields vary and the shielding nature of the superconductor is overwhelmed by the local Lorentz force acting on the pinned vortices. Although in most cases the superconductor can recover from such events, the resulting flux dynamics cause small field fluctuations that must be minimised.

These issues are addressed by minimising the effective diameter of the filaments. This is an area of active development by industry, with support from the CDP in the US. We note that the HTS materials Bi-2212 and YBCO currently suffer both from large effective filament sizes. Significant advances will need to occur in the material technology for the conductors to be viable candidates for accelerator dipoles. Other magnet systems, such as interaction region (IR) quadrupoles and solenoids for a muon accelerator, are much less sensitive to field quality concerns and may be early adopters of HTS materials. The use of high T_c conductors gives an important temperature margin to these systems and needs to be a priority in the R&D program.

In terms of magnet design, field quality is dictated by the conductor layout in the coil cross-section, a fairly well understood area. Open issues include a thorough understanding of fabrication and assembly tolerances and their impact on field quality and the understanding of the influence of thermal contraction and deflections associated with magnet energization, and their impact on field quality.

5.4. Collimation

The LHC collimation system is operating well, but in order to cope with the higher beam energy density as well as to lower impedance it will need to be renovated. Gains in triplet aperture and performance must be matched by an adequate consolidation or modification of the collimation system. In addition, a collimation system in the dispersion suppressor (DS) needs to be added to avoid the leakage of off-momentum particle, into the first and second main SC dipoles. This has been already identified as a possible LHC performance limitation. The most promising proposed concept requires the substitution of one of the LHC main dipoles with a dipole of equal bending strength (121 T-m) of shorter length (11 m) and higher field (11 T) than those of the present LHC dipoles (8.3 T and 14.2 m). The gain in space is sufficient to place special collimators to intercept the off-momentum particles. This new 11 T dipole, which is jointly developed by CERN and Fermilab, will be actually realised with two cold masses of 5.5 m length, and should become the first magnet breaking through the 10 T frontier to be installed in a particle accelerator. The higher energies and beam intensities contemplated for a future proton collider set even more challenging requirements on the collimation system which need to be addressed. The collimation system being developed for the HL-LHC will represent the knowledge base for a future machine, given the energy density scaling of log E with the beam energy, E.

5.5. Crab cavities

In order to preserve the luminosity for beams colliding at a large crossing angle, the beams can be rotated before, and after, collision using dedicated RF resonators known as crab cavities [48]. Crab cavities have been successfully developed and installed at the KEKB b factory [49]. The crab cavities foreseen for the HL-LHC upgrade are not particularly demanding in terms of the required voltage. However, they go beyond the state-of-the art because the transverse cavity dimension is limited by the small distance between the two LHC beams (194 mm), which is smaller than the $\lambda/4$ value of the 400 MHz wave. This practically excludes the elliptical cavity geometry adopted at KEKB. The need for small beam separation requires an unconventional, very compact design

Fig. 17. The three types of compact crab cavities under development for HL-LHC.

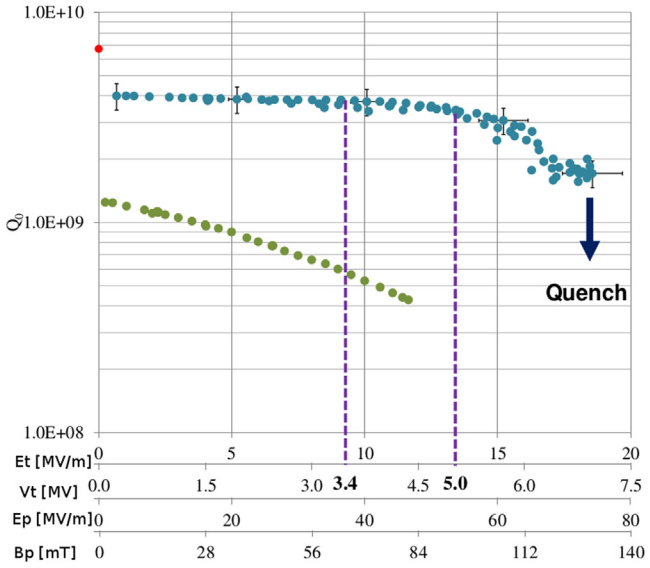

Fig. 18. Results of the first full test of a crab cavity: the RF dipole Nb prototype (ODU-SLAC, LARP). The vertical lines show the target voltage (3.4 MV) and the actual usable voltage (5 MV). Beside the transverse gradient and voltage, on the horizontal axis, the peak electric field and magnetic field are indicated. The test has been carried out at JLab.

for the HL-LHC crab cavities. Looking for such an unconventional design approach, different options have been proposed. After detailed studies and R&D three design candidates have emerged and are being developed through prototypes, shown in Fig. 17.

The first full test of a cavity prototype has just been completed for the RF-dipole type. It was operated well above the target value of 3.4 MV transverse voltage V_T (see Fig. 18), quenching at 7 MV and showing operational gradient at 5 MV. This result is very encouraging, though issues remain to be addressed. General critical issues for the use of crab cavities include their effect on the proton beam in term of noise-induced beam emittance growth and the understanding of possible failure modes, which must be carefully studied in order to allow the safe operation of the machine. Then the cavity integration in a very compact cryostat must be addressed. Since beam crabbing with protons is not yet proven, a beam test in the SPS is planned before the LS2 shutdown of the LHC. This test will offer an opportunity to evaluate the use of crab cavities with proton beams,and have a better understanding of the feasibility of such a system and its implementation in the HL-LHC.

The possibility of adopting crab cavities at the HL-LHC is not yet fully demonstrated. Should the use of crab cavities not be feasible, the loss in luminosity can be minimised by changing the beam parameters to collide flat beams at the smallest possible crossing angle, by pushing the compensation for the Long-Range beam-beam interactions by installing compensating conducting wires, where the current counteracts in part the beam-beam effects.

6. Higher energy colliders

Given the progress in magnet technology and the maturity that Nb_3Sn is reaching, thanks to its development for the HL-LHC, it is legitimate to forecast that Nb_3Sn magnets can reach their limit of 14–16 T with 15–20% margin in operative condition within the next decade, opening the path towards future circular colliders with energy significantly larger than that of the LHC, which bring an exceptional potential for probing the energy frontier of particle physics.

6.1. HE-LHC

The first option being considered is a machine housed in the present LHC tunnel (HE-LHC). The achievable centre-of-mass energy depends on the dipole field strength. An energy of 26 TeV is within reach using Nb_3Sn technology magnet, which offers a big advantage in reducing complexity and cost of the magnet system. The centre-of-mass energy would become ~33 TeV, if 20 T magnets were available, which would require the use of more futuristic HTS conductors. In this case, the limited space available in the LHC tunnel represents an important challenge to overcome. The inter-beam distance must be increased to 300 mm in order to allow for thicker superconducting coils in the main dipoles and quadrupoles in order to generate the 20 T field. A 2D design of the magnet featuring an aperture of 40 mm and an operative field of 20 T with realistic overall current density in all coils block (J_E=400 A/mm^2) has been initiated. Anti-coils are needed to reduce stray field, collider field quality is not yet proved and magnet powering and protection will be certainly an issue. A vigorous R&D program is needed to demonstrate the viability of HTS-based cables and the subsequent magnet engineering design. In fact, the inner block of HTS adds about 4–5 T, and it is necessary for the 20 T target.

The beam parameters for the HE-LHC are not too different from those for the LHC or HL-LHC. In this respect the machine design looks feasible [4,50]. However, there are two areas which have been identified as critical, in addition to the magnets. First, the injection scheme relies on kickers more powerful than those used at LHC, which are already at the limit of current technology. The extraction system is also critical, though to a lesser extent. An important program of R&D in fast-pulsed, high-strength kickers is a necessary complement to the dipole magnet program. Then, the beam pipe and beam screen have to absorb a synchrotron radiation which is more than 20 times higher than the LHC. Synchrotron radiation is very beneficial for beam stabilisation and would make the HE-LHC the first hadron machine dominated by synchrotron radiation damping. However, the power dissipated in SR must be removed at cryogenic temperature. In LHC it is removed at 5–10 K. A similar solution with a beam screen at 10 K will be a heavy burden for the cryogenics. The additional 12 kW of power needed for each of the eight sectors would require roughly doubling the present 8×18 kW cryoplants. In addition, the beam screen refrigeration would be complicated by the need to increase the local heat removal by a factor of 20 by increasing the pressure drop and the conductance of the cooling pipe. Although this solution should be possible, better options seem to be available.

The first option would be to remove the SR heat at higher temperature. Vacuum stability indicates two possible windows for beam screen operation: 40–60 K (inlet–outlet temperature) and 85–100 K. The first window of operation would maintain the cryogenic power at 4.2 K to be equal to that of the LHC; the second window would make refrigeration easier than in the baseline LHC. However, the first option is preferable because in the second option the heat leakage from a higher temperature beam screen onto the 1.8 K cold mass would be more than double that of the first option. Moreover the electrical resistivity increases by a factor of 5 above the LHC value for the first option and a factor of 22 for the higher temperature window.

The consequences of the higher resistivity on beam stability are not dramatic, because both transverse and longitudinal beam impedance increase with the square root of the wall resistivity. The resistivity of copper at 50 K and 20 T is just a factor 2.5 more than the resistivity at 20 K, 8.3 T, resulting in an impedance increase of just 60%, a manageable factor. A copper coating thicker than the 75 μm used in LHC will partially compensate the

increased resistivity, a compensation that is necessary to cut down power losses due to image currents.

Although a copper coating appears to be a viable solution for HE-LHC, the use of coating with YBCO (T_c=85 K) or Bi-2223 (T_c=110 K) on the inner surface of the beam screen (if practical) could virtually null the resistance, eliminating the problem. The HTS coating will even make possible working at 100 K (if the thermal contact to the 1.9 K cold mass can be made tiny enough). This HTS coating will certainly be more expensive and complex that the copper-stainless steel co-lamination of the LHC beam screen. However, given its potential benefits, it should be carefully investigated as part of this R&D program.

6.2. Proton colliders beyond LHC

Studies for a very large future circular collider able to deliver pp collisions at centre-of-mass energies of order of 100 TeV (and more) have been already conducted since the mid-1980s and subsequently updated, in a detailed multi-laboratory study led by Fermilab [51], recently updated with the use of higher field magnets [12]. A study to investigate the feasibility of a 80–100 km future circular collider (FCC) ring driven by the requirements of a next-generation hadron collider is now starting at CERN, with the aim to produce a complete machine conceptual design by 2018.

The construction of a new tunnel relieves the pressure on the achievable dipole field strength, since this can be traded for the tunnel circumference. The target collision energy for the FCC is 100 TeV for 20 T dipoles in an 80 km tunnel. However, a 100 km tunnel would provide the same collision energy of 100 TeV with reduced field of 16 T, reachable with Nb_3Sn technology which uses a much more mature and less expensive conductor than HTS. The CERN civil engineer team has studied a 5 m diameter tunnel, compared to the 3.8 m of the present LHC tunnel, thus allowing for larger cryo-modules. Cost and magnet technology put aside, the main issue for this collider is the removal of synchrotron radiation. In a 80 km, 100 TeV proton collider, the dumped SR power will jump from the 3.6 kW/ring of the LHC and 82 kW/ring of a HE-LHC to ~2 MW/ring. Dealing with this 500 times increase of SR compared to the present LHC value will be a major issue. While the beam stabilisation will get a tremendous benefit, making the machine much easier from the point of view of the beam dynamics, we do not know if a beam screen cooled at 100 K (to limit thermodynamic load) would be capable of withstanding the resulting heat deposition. Furthermore, the critical energy of the emitted photon is in the soft X-ray range and its impact on the *e*-cloud effect and surface needs to be studied. The issue of synchrotron radiation removal is key to the machine feasibility. The design of the vacuum system is a central R&D issue that has the potential to have a very large impact on the overall collider design. The limits of cost-effective handling synchrotron radiation power in ultra-high vacuum systems at cryogenic temperatures are not known experimentally. A primary component of the vacuum system is the beam screen which must provide good vacuum yet sufficiently small impedance for the beam while efficiently removing the high synchrotron radiation heat load (up to a maximum of 44 W/m/beam, a total of around 5 MW) and shielding the magnets. The vacuum system must cope with a strong variation of the heat load during the ramp. At the same time the space used for the screen has to be minimised to limit the magnet aperture, which is one of the main cost drivers.

The first option would be to operate the beam screen in the temperature window of 85–100 K, suitable for vacuum stability. However, assuming an efficiency between cryo power and plug power of 10%, the 2×2 MW power removed at 90 K implies a requirement of approximately 2×20 MW for the cryogenic plant. Since the cryogenic power for the full ring is of the order of 120 MW (for 1.9 K magnets) or 40 MW (for 4.2 K magnets), the additional power consumption of 40 MW for removal of synchrotron radiation remains acceptable. However, the problem of keeping the beam screen well insulated (at 100 K) from the vacuum pipe (at 1.9 or 4.2 K) while removing longitudinally the 37 W/m inside the vacuum pipe represents a major challenge. The cooling pipe of the beam screen may become too large and require an increased magnet aperture, beyond the 40 mm, that has been the guideline for the HE-LHC and FCC-hh magnet concepts, so far. Another possible solution is to investigate the possibility of letting the radiation escaping from the beam pipe and intercept it with cold fingers (or photons stops) at a temperature to be optimised in the range between 80 K and room temperature, as proposed in the US VLHC study [52]. In the case the cold finger is kept at 80 K, the cryogenic load of 40 MW will remain, however the issue of local removal of the heat along the beam screen is avoided. The magnet aperture might still need to be increased. A detailed study and optimisation, which includes the length of the main dipoles, should establish the best solution. Although the problem of synchrotron radiation is challenging, it should not been considered to be a showstopper. The benefit of the strong damping due the synchrotron radiation at 50 TeV/beam should be underlined. Transverse damping time becomes about 30 min, to be compared to one day at the LHC, and this will greatly contribute to resolving the issue of beam stability due to impedance or other collective effects. The coating of the beam screen with HTS, as proposed for a HE-LHC, may be not required for a long tunnel. The cryogenic system will have to be much more powerful than that installed at the LHC, because of the tunnel length and of the dumped SR power. It will represent a cost driver and will seriously impact the facility power consumption. A very preliminary estimate of the electrical power needed for the cryo-system is in the range of 150–200 MW. The generation of electron clouds from synchrotron radiation must be suppressed. The vacuum system must also deal with pressure burst and ions. Additional challenges are the large size of the system and the high radiation environment. The so-called UFOs (Unidentified Falling Objects), which are probably caused by dust particles, have impacted the LHC operation; one needs to find methods to avoid them in the FCC. The development of a model of the arc beam pipe system, and experimental verification its performance in the presence realistic synchrotron radiation environments and with ideally with positively charged beams for measuring electron cloud effects should be made early in a study of a 100 TeV class collider. CESR-TA at Cornell could provide an appropriate test infrastructure. Theoretical studies are required both to optimise the system design and to evaluate the experimental data. Such studies should include the propagation and capture of the synchrotron radiation and the generation of secondary electrons.

The study of a high energy hadron collider will capitalise on experience gained in the HL-LHC R&D and guide the long-term roadmap with strong synergies with other programs, such as muon acceleration and and high intensity machines.

7. Conclusions

High energy hadron colliders have been key to the progress of particle physics at the high energy frontier, from the discovery at the W and Z bosons at the $S\bar{p}pS$ to that of the top quark at the Tevatron and now of a Higgs-like scalar boson at the LHC. The full exploitation of the LHC is currently the highest priority of the energy frontier collider program. The high luminosity LHC will represent a new phase of the LHC life preparing the collider to reach 3000 fb^{-1} of integrated luminosity during its first decade of operation.

In view of the practical limitation with the beam current and frequency, the chosen route for increasing the LHC luminosity is the reduction of the beam focusing at the IP, β^*. In order to be compatible with the reduced β^* values, both the aperture of the low-β^* quadrupole magnets and the peak field need to be doubled, thus requiring a new superconducting magnet technology, which will be based on the Nb_3Sn conductor.

Given the progress in magnet technology and the maturity that Nb_3Sn has reached through the HL-LHC R&D, it is now legitimate to forecast that Nb_3Sn magnets can reach their limit of 14–16 T in operative condition within the next decade, thus opening the path towards a collider with energy significantly larger than that of the LHC, with an exceptional potential for further probing the energy frontier.

The continuation of an international R&D program towards the engineering development of higher field magnets is essential to the development of the design for an HE-LHC in the LHC tunnel or a new collider of higher energy in a larger tunnel. Such a program of innovative engineering should establish the limits of the Nb_3Sn technology, reduce the operating margin required for operation, investigate new conductor materials and re-assess our present concept for managing the enormous stresses produced by such high magnetic fields. The experience from HERA, RHIC, Tevatron, SSC and LHC indicates that the dipoles account for about half of the total collider cost. Therefore, magnet technology is an area of critical investment and should represent a major focus of the R&D process, as is was discussed extensively in this review. A new generation of magnets using high temperature superconductors will require new engineering materials with small filament size and available in multi-kilometre piece lengths. Advanced magnets may offer greater temperature margin against quenches due to stray radiation lost from the beam. Higher field magnets will require proven stress management techniques, exquisitely sensitive magnet protection schemes, and perhaps novel structural materials. Beam dynamics and other effects of marginal (as compared with electron colliders) synchrotron radiation damping must be understood. As the energy stored in the machine reaches several gigajoules, control of tenuous beam halos becomes a pressing issue. Likewise machine protection from accidental beam loss and the design of special beam abort dumps becomes a difficult challenge that requires innovative approaches.

Considering the LHC tunnel, an energy of 26 TeV is within the reach of a focused engineering readiness program on Nb_3Sn technology, although it still requires significant engineering development. The energy reach would become $\sim$33 TeV, if 20 T magnets based on futuristic high temperature superconductors were practical and affordable and if the constraints imposed by the limited space available in the LHC tunnel could be overcome. Beyond the confines of the LHC tunnel, a $\sim$100 TeV proton collider would become possible in a larger tunnel. Studies for a very large proton collider able to deliver centre-of-mass energies of that scale have already been conducted over the past two decades and will now be stepped up towards a conceptual design report for a future circular collider, driven by the pp requirements (FCC-hh) with the possibility of providing also e^+e^- (FCC-ee) and pe^- collisions (FCC-eh).

Whether in the LHC tunnel or in a new, larger tunnel, a future circular collider with energy beyond the LHC will have to deal with additional challenges, in particular the large power radiated by the beam in synchrotron radiation. The beam pipe and beam screen will have to absorb that radiation. Although synchrotron radiation is very beneficial for beam stabilisation and will make this collider the first hadron machine dominated by synchrotron radiation damping, the power dissipated must be removed at cryogenic temperatures. Although the problem of synchrotron radiation is challenging, it should not been considered to be a showstopper.

Other issues that should not be neglected in a long range R&D program include beam physics of the injection chain, noise and ground motion effects, and the design and technology options for the configuration of the interaction regions. Advanced instrumentation provides us with detectors which are faster, thinner and have higher segmentation. Their application to imaging for beam monitoring and diagnostics should be carefully considered. These R&D areas have all substantial implications for lepton colliders and the intensity frontier program.

High energy hadron collisions have produced some of the most fruitful collider physics research and the LHC program will extend this trend over the next decade, or more. In order to maximise the potential for discovery in the farther future, this collider program requires a sustained, long-term R&D effort.

Acknowledgments

This review is based on the report of the Frontier Capabilities Hadron Collider study group in the APS Community Summer Study – CSS 2013. We thank G. Apolllinari, M. Benedikt, S. Bertolucci, P.C. Bhat, L. Brouwer, S. Caspi, A. Ratti, G.L. Sabbi and F. Zimmermann for their comments and contributions, D. d'Enterria and E. Todesco for providing some of the figures.

References

[1] G. Aad, et al., ATLAS Collaboration, Physics Letters B 716 (2012) 1 arxiv:1207.7214[hep-ex].
[2] S. Chatrchyan, et al., CMS Collaboration, Physics Letters B 716 (2012) 30 arxiv:1207.7235[hep-ex].
[3] F. Zimmermann, O. Brüning, in: Proceedings of the IPAC-2012, New Orleans.
[4] E. Todesco, F. Zimmermann (Eds.), Report CERN-2011-003, 2011.
[5] C.O. Dominguez, F. Zimmermann, in: Proceedings of the IPAC-2013, Shanghai.
[6] ATLAS Collaboration, ATL-PHYS-PUB-2012-004.
[7] CMS Collaboration, arxiv:1307.7135[hep-ex].
[8] F. Zimmermann, EuCARD-CON-2011-002.
[9] The European Strategy for Particle Physics, Update 2013, CERN-Council-S/106, 2013.
[10] P. Wanderer, IEEE Transactions on Applied Superconductivity 19 (2009) 1208.
[11] O. Bruning, et al., EuCARD-CON-2013-008.
[12] C.M. Bhat, et al., FERMILAB–CONF-13-195-AD-APC-PPD, arxiv:1306.2369[physics.acc-ph].
[13] T. Sen, J. Norem, Physical Review Special Topic on Accelerators and Beams 5 (2002) 031001.
[14] M. Koratzinos, et al., arxiv:1305.6498[physics.acc-ph].
[15] Higgs Cross-Section WG, in: Submission to the Krakow Symposium of the European Strategy Group, ⟨https://indico.cern.ch/contributionDisplay.py?contribId=176&confId=175067⟩.
[16] P.Z. Skands, arxiv:1308.2813[hep-ph].
[17] A. Donnachie, P.V. Landshoff, Physics Letters B 296 (1992) 227 [hep-ph/9209205].
[18] G.A. Schuler, T. Sjostrand, Physical Review D 49 (1994) 2257.
[19] T. Sjostrand, S. Mrenna, P.Z. Skands, Journal of High Energy Physics 0605 (2006) 026 [hep-ph/0603175].
[20] B. Abelev, et al., ALICE Collaboration, European Physics Journal C 73 (2013) 2456 arxiv:1208.4968[hep-ex].
[21] D. d'Enterria, et al., Astroparticle Physics 35 (2011) 98 arxiv:1101.5596[astro-ph.HE].
[22] P.Z. Skands, Physical Review D 82 (2010) 074018 arxiv:1005.3457[hep-ph].
[23] G. Aad, et al., ATLAS Collaboration, Journal of High Energy Physics 1211 (2012) 033 arxiv:1208.6256[hep-ex].
[24] A. Karneyeu, L. Mijovic, S. Prestel, P.Z. Skands, arxiv:1306.3436[hep-ph].
[25] S. Chatrchyan, et al., CMS Collaboration, Journal of High Energy Physics 1111 (2011) 148 [Erratum-ibid. 1202 (2012) 055] [arxiv:1110.0211[hep-ex].
[26] G. Antchev, et al., TOTEM Collaboration, Europhysics Letters 98 (2012) 31002 arxiv:1205.4105[hep-ex].
[27] S. Fartoukh, Physical Review Special Topic on Accelerators and Beams 16 (2013) 111002.
[28] R. Calaga, et al., Conference Proceedings C 070625 (2007) 1853.
[29] R. De Maria, S.D. Fartoukh, Conference Proceedings C 110904 (2011) 3712.
[30] L. Rossi, CERN AT/2003-2.
[31] B.P. Strauss, S.J.St. Lorant, IEEE Transactions on Applied Superconductors 21 (3) (2010) 936.
[32] D.F. Sutter, B.P. Strauss, IEEE Transactions on Applied Superconductors 10 (1) (2002) 33.
[33] P. Ferracin, AIP Conference Proceedings 1218 (2010) 1291.

[34] L. Bottura, G. de Rjik, E. Todesco, L. Rossi, IEEE Transactions on Applied Superconductors 22 (3) (2012).
[35] E. Todesco, P. Ferracin, Report CERN-ATS-2012-052.
[36] G.L. Sabbi, et al., IEEE Transactions on Applied Superconductivity 12 (1) (2002) 236.
[37] A. Godeke, et al., IEEE Transactions on Applied Superconductivity 17 (2) (2007) 1149.
[38] R.M. Scanlan, IEEE Transactions on Applied Superconductors 11 (1) (2001) 2150.
[39] A. Godeke, et al., Superconductor Science and Technology 23 (2010) 034022.
[40] H.W. Weijers, et al., IEEE Transactions on Applied Superconductivity 20 (3) (2010) 576.
[41] D.C. Larbalestier, et al., arxiv:1305.1269[cond-mat.supr-con].
[42] T. Shen, et al., Journal of Applied Physics 113 (2013) 213901.
[43] D.C. Larbalestier, et al., Nature Materials 13 (4) (2014) 375.
[44] L. Rossi, O. Bruning, Report CERN-ATS-2012-236.
[45] T. Elliot, et al., IEEE Transactions on Applied Superconductivity 7 (2) (1997) 555.
[46] D.I. Meyer, R. Flasck, Nuclear Instruments and Methods in Physics Research 80 (1970) 339.
[47] L. Rossi, E. Todesco, Report CERN-2011-003.
[48] R.B. Palmer, eConf C 8806271 (1988) 613.
[49] K. Hosoyama, et al., Conference Proceedings C 0806233 (2008) THXM02.
[50] O. Bruning, et al., Report CERN-ATS-2012-237.
[51] Design Study for a Staged VLHC, Report Fermilab TM-2149, 2001.
[52] M. Pivi, W.C. Turner, P. Bauer, P. Limon, Conference Proceedings C 0106181 (2001) 613.